

Reliable Multimedia Transmission Over Cognitive Radio Networks Using Fountain Codes

By sensing spectrum use and carefully controlling access, multimedia data transmissions can be squeezed into temporarily-unused parts of the radio spectrum without interfering with licensed spectrum users.

By HARIKESHWAR KUSHWAHA, *Student Member IEEE*, YIPING XING, *Student Member IEEE*, RAJARATHNAM CHANDRAMOULI, *Senior Member IEEE*, AND HARRY HEFFES, *Fellow IEEE*

ABSTRACT | With the explosive growth of wireless multimedia applications over the wireless Internet in recent years, the demand for radio spectral resources has increased significantly. In order to meet the quality of service, delay, and large bandwidth requirements, various techniques such as source and channel coding, distributed streaming, multicast etc. have been considered. In this paper, we propose a technique for distributed multimedia transmission over the secondary user network, which makes use of opportunistic spectrum access with the help of cognitive radios. We use digital fountain codes to distribute the multimedia content over unused spectrum and also to compensate for the loss incurred due to primary user interference. Primary user traffic is modelled as a Poisson process. We develop the techniques to select appropriate channels and study the trade-offs between link reliability, spectral efficiency and coding overhead. Simulation results are presented for the secondary spectrum access model.

KEYWORDS | Cognitive radio; distributed streaming; LT codes; Poisson model; secondary spectrum access

Manuscript received October 30, 2006; revised June 13, 2007. This work was supported by the National Science Foundation under CAREER Grant 0133761.

H. Kushwaha, R. Chandramouli, and H. Heffes are with the Department of Electrical and Computer Engineering, Stevens Institute of Technology, Hoboken, NJ 07030 USA (e-mail: hkushwah@stevens.edu; mouli@stevens.edu; hheffes@stevens.edu).

Y. Xing was with the Department of Electrical and Computer Engineering, Stevens Institute of Technology, Hoboken, NJ 07030 USA. He is now with Bear Stearns, New York, NY 10179 USA (e-mail: YXing@bear.com).

Digital Object Identifier: 10.1109/JPROC.2007.909917

I. INTRODUCTION

Wireless multimedia applications require significant bandwidth and often have to satisfy relatively tight delay constraints. Radio spectrum is a scarce resource. Limited available bandwidth is considered one of the major bottlenecks for high-quality multimedia wireless services. A reason for this is the fact that a major portion of the spectrum has already been allocated. On the other hand, actual measurements taken on the 0–6 GHz band in downtown Berkeley [2] and other spectrum occupancy measurements on licensed bands, such as TV bands, show the significant under utilization of the spectrum [3], [4].

Recent Federal Communications Commission (FCC) proceedings [5] propose the notion of secondary spectrum access to improve spectrum utilization. This allows dynamic access to the unused parts of the spectrum owned by the primary license holder, called a primary user (PU), to become available temporarily for a secondary (nonprimary) user (SU). This dynamic access of spectrum by secondary users, which is facilitated by the use of cognitive radios [6], is one of the promising ideas that can mitigate spectrum scarcity, potentially without major changes to incumbents. Fortunately, the advances in software defined radio (SDR) [6], [7] have enabled the development of flexible and powerful radio interfaces for supporting spectral agility.

Cognitive radio is a wireless communication paradigm in which either the network or the wireless node itself changes particular transmission or reception parameters to execute its tasks efficiently without interfering with the

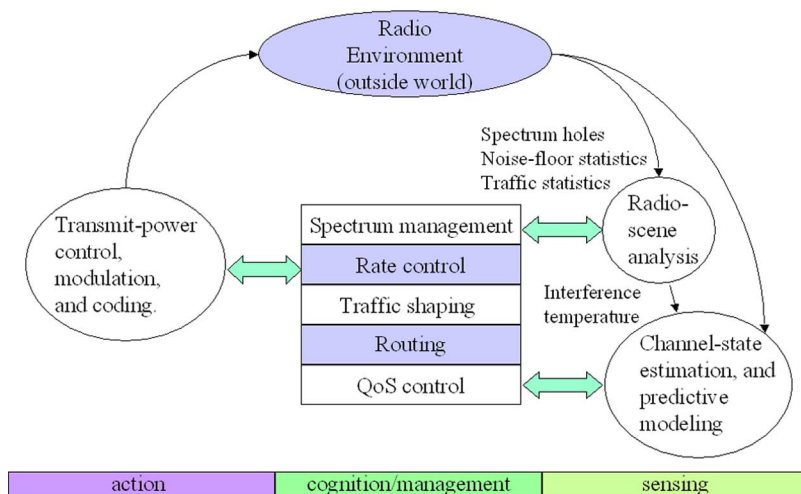


Fig. 1. Basic cognitive cycle.

licensed users or other cognitive radios. This parameter adaptation is based on several factors, such as the operating radio-frequency (RF) spectrum, user behavior, and network state. A cognitive radio may depend on a software-defined radio to implement the functionality to support reconfiguration. The cognitive radio also looks at signal-processing and machine-learning procedures from the algorithmic perspective. The cognitive cycle consists of three major components: *sensing of RF stimuli*, *cognition/management*, and *action*.

- 1) Sensing of RF stimuli encompasses the following:
 - detection of spectrum holes;
 - estimation of channel state information;
 - prediction of channel capacity for use by the transmitter.
 - estimation of interference temperature (maximum allowable interference in a band) of the radio environment. Note that the FCC abandoned the interference temperature concept recently.¹
- 2) Cognition/spectrum management includes:
 - spectrum management, which controls opportunistic spectrum access;
 - optimal transmission rate control;
 - traffic shaping;
 - routing;
 - quality of service provision.
- 3) Examples of actions are:
 - transmit-power control, adaptive modulation, and coding.

These three tasks form a cognitive cycle as shown in Fig. 1. For additional information about the cognitive cycle, we refer to [1].

¹http://hraunfoss.fcc.gov/edocs_public/attachmatch/FCC-07-78A1.doc.

In our model, we use the spectrum pooling concept [8] to select a set of subchannels (SC) in order to establish a communication link. Cognitive radio networks do not require the selected subchannels or bands to be contiguous. Thus, a cognitive radio can send packets over non-contiguous spectrum bands. Since a link is composed of multiple different SCs at different frequencies, it adds path diversity in the network, and thus helps in achieving distributed streaming of the multimedia content through multiple paths with a higher overall throughput to the client. For example, it has been shown in [9] that the usage of multiple streaming servers provide better robustness in case one of the channels becomes congested. The multiband spectral diversity also helps to improve the reliability of secondary spectrum access. For example, if a primary user appears in a particular spectral band, the secondary user has to vacate this band. The other available bands, in this situation, will still help in secondary link maintenance.

However, the inherent problem of distributing media over multiple SCs is the coordination required between the SCs. Packet scheduling strategies need to be carefully coordinated in order to efficiently utilize the scarce spectral resources. This could make such a distributed streaming system overly complex and cumbersome, especially in a secondary user environment where primary user arrival is unpredictable.

In this paper, similar to [10], we propose to make use of digital fountain codes in order to remedy the aforementioned coordination problems. In fact, the use of fountain codes achieves two goals simultaneously. First, it renders it feasible to distribute the scalable media to different SCs with no need of coordination between them. Secondly, it acts as a channel code to combat the effect of loss against PU interference and other channel conditions. Fountain codes are a class of erasure-correcting codes that produce

an endless supply of packets from a set of K input packets, out of which any N packets can be used to recover the original K packets with a certain probability of error ϵ , where N is slightly greater than K . In order to transmit K packets of data, a redundancy approach has been used in [11] and [12], where some redundancy X is used to compensate for the loss due to PU interference. So a total $N + X$ packets are distributed over a set of S SCs.

The problem of how to select the set of appropriate SCs to meet the quality of service (QoS) requirements of the multimedia communication is of great interest and still an open problem [13]. In this paper, we propose a novel metric to evaluate the quality of different SCs. The encoded packets are distributively transmitted through multiple subchannels selected from the spectrum pool based on the new channel quality metric and the QoS requirement of the media steaming application. Theoretic analysis is presented to show that the proposed method will optimally allocate the data rate to different subchannels to achieve the target requirement. In this paper, we model primary user arrival as a Poisson process whose parameter λ can be estimated by a maximum likelihood estimator. Some measurement studies also support the Poisson model [24], [25]. We also discuss other possible modeling of the primary user traffic such as the Markov chain [26]. We use these models to investigate the spectrum efficiency of the SU link with respect to the PU arrival rate and the number of selected subchannels S . We also study the tradeoff between λ and S .

The rest of this paper is organized as follows. In Section II, we describe the spectrum pooling concept and PU arrival process. We also discuss the digital fountain codes and the coding scheme for distributed multimedia applications. In Section III, we discuss various techniques for estimating PU arrival rate and channel errors. In Section IV, our problem description and theoretical analysis are presented. Simulation results and performance analysis are presented in Section V. Section VI presents concluding remarks.

II. SYSTEM MODEL

In this section, we first introduce the spectrum pooling concept. This is the basis for our secondary usage model used for finding out vacant channels to be considered for distributing multimedia contents over them. Then we describe the PU arrival model, and after that digital fountain codes, which are used to distribute the multimedia contents over different SCs that help in compensating for the PU interference.

A. Spectrum Pooling Concept

In the secondary usage scenario, the availability of the radio spectrum is dependent on the PUs' usage statistics. So in order to transmit multimedia content, first we need to isolate a portion of the radio spectrum that is not in use

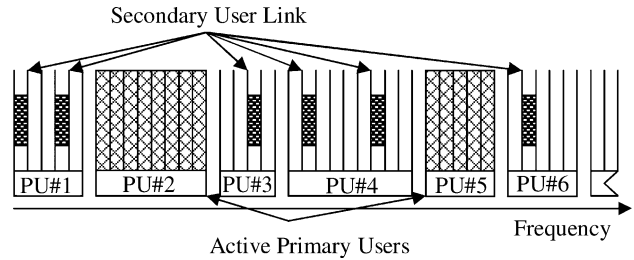


Fig. 2. Spectrum pooling concept.

by the primary users. Similar to [12], we use the spectrum pooling concept as shown in Fig. 2, which is the basis for the secondary usage system architecture called *cognitive radio for virtual unlicensed spectrum (CORVUS)*, as described in [2]. Since PUs use their bands intermittently, SUs get the opportunity to exploit the temporarily available spectral resources to accomplish their own communication needs.

In Fig. 2, the whole spectrum where secondary use is permitted is divided into many SCs of bandwidth W . The SU selects a set of SCs (say, S) to form an SU link in such a way that the interference due to PU is minimized. For example, if one subchannel is selected per PU band then the arrival of a PU will not cause the complete breakdown of the SU link, rather the link will degrade gradually.

B. Primary User Arrival Model

We consider a compressed video transmission application for the secondary user. The video data consists of a group of pictures (GOP). At the start of every GOP, an SU link is set up by selecting a set of S subchannels out of S_0 available subchannels from different PU bands of the spectrum pool. Then the SU starts transmitting packets over this link at $t = 0$. The GOP frame structure is shown in Fig. 3. The PU arrival process on SC i , for $i = 1, 2, \dots, S_0$, is modelled as a Poisson process with arrival rate λ_i . So the interarrival time τ_i is exponentially distributed with mean-arrival time $\mu_i = 1/\lambda_i$, as shown in Fig. 4. Each SC has a loss probability π_i and channel capacity R_i .

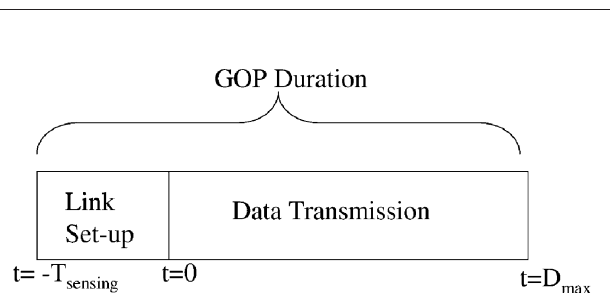


Fig. 3. GOP frame structure.

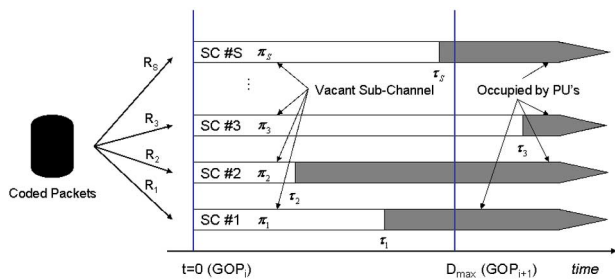


Fig. 4. Subchannel access model.

If the i th subchannel is reclaimed by the primary user at time τ_i , then all packets transmitted on that subchannel after τ_i will be lost due to the evacuation of the secondary user. So in order to recover these packets, some error-correcting mechanisms are needed. One method is to request for retransmission (i.e., ARQ), for which a feedback channel is required. However, in this secondary access scenario, once the subchannel has been captured by a primary user, the retransmission request has to be placed on a different subchannel, which may not be available or reliable. So in order to avoid the need for a feedback channel, we propose to use erasure-correcting codes, where the packets that are lost due to PU interference are considered as erasures. The erasure-correcting codes that we use in our model are digital fountain codes and are discussed next.

C. Digital Fountain Codes

The theoretical idea of digital fountain codes was introduced in [14], and the first practical realizations of fountain codes were invented by Luby [15]. They represent a new class of erasure-correcting codes for packet data transmission over lossy channels.

For a given set of input packets $\{x_1, x_2, \dots, x_K\}$, a Luby transform (LT) [15] code can generate a limitless stream of output packets. Each output packet is generated independently by first choosing a degree d from a distribution $\Omega(k)$, where $k \in \{1, 2, \dots, K\}$, on the set $\{1, 2, \dots, K\}$, then randomly selecting d input packets from $\{x_1, x_2, \dots, x_K\}$ followed by addition of the d selected input packets. The connections between the input packets and output packets form a bipartite graph. An example graph is shown in Fig. 5. The sequence of output packets along with this graph is transmitted over the lossy channel. Once N of the output packets, where N is slightly more than K , has been received, irrespective of which N packets, a belief-propagation decoder is applied to decode the original K input packets. The choice of N depends on the LT code parameters $(K, \Omega(k))$ and the desired error probability (ϵ) of the decoder.

Since the LT decoder only needs any N output packets to recover original K input packets with probability $1-\epsilon$, irrespective of the loss model of the channel, it is robust

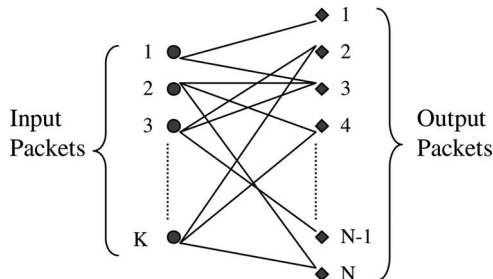


Fig. 5. Bipartite graph representing the LT code.

against the packet loss caused by the PU interference. But if the PU interference is high, then it will cause additional delay to receive the correct N output packets for decoding to begin. In our model, if, out of S SCs, some of them are occupied by PUs during transmission, then the decoder waits longer to receive the N packets on the remaining SCs. But for multimedia applications, which are delay-constrained, if the decoder does not receive N packets within D_{max} , the maximum tolerable delay as shown in Fig. 4, then it results in a decoding error. In order to receive N packets with a high probability, we can increase the number of SCs, which will distribute the N packets over a larger number of SCs, thereby reducing the average required packets per subchannel. Therefore, depending upon the PU arrival rate (λ) , we can optimize the number of SCs that will give the maximum effective throughput and spectral efficiency.

Another class of fountain codes called *raptor codes* was developed by Shokrollahi [16]. Raptor codes are an extension of LT codes with linear time encoding and decoding complexity. This is accomplished by first precoding the source data by an appropriate outer code to generate the input packets for the LT code, as shown in Fig. 6.

D. Coding Scheme for Scalable Multimedia Applications

We first note that blindly applying a fountain code on a media bitstream would mix the time dependencies and the intralayer dependencies that are present in the original scalable media stream. Similar to [10], we propose to create one fountain per layer and per GOP of the original bitstream, as depicted in Fig. 7. Such a fountain is denoted \mathcal{F}_l^t , where l stands for the layer, $1 \leq l \leq L$, and t is the timestamp associated with the corresponding GOP. It encodes a set of K_l^t source symbols, which depends on the

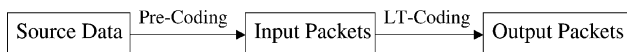


Fig. 6. Raptor codes schematic.

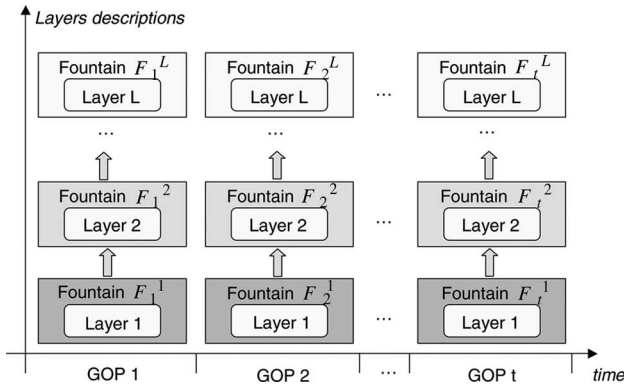


Fig. 7. Coding scheme: a fountain is created per GOP and per layer. The vertical arrows show the hierarchical dependence in the bitstream.

encoding rate of the layer l . Such a coding scheme allows keeping the hierarchical and temporal dependencies present in the original bitstream, which are essential for the scalable delivery of the stream. Then, each selected subchannel is used to send different packets from the same fountain \mathcal{F}_i^l , such that the receiver does not receive any duplicated packets.

III. PRIMARY TRAFFIC MODELING AND PARAMETER ESTIMATION

A. Arrival Traffic Rate Estimation

Depending on the types of primary users, the primary traffic model may be different. For instance, when the primary users are TV channels as proposed in IEEE 802.22 [19], the traffic pattern will tend to be bursty. This comes from the fact that TV programs broadcast according to predetermined schedules. When the programs are terminated, the off-air period will last for a relatively long period of time. Hence, these traffic conditions can be modelled by a Markov process as presented in [17], where the assumption is that each channel independently presents itself as an opportunity to a secondary user according to a Markov process when the network reaches a steady state. The channel states are represented by 0 (busy) and 1 (idle and available to the secondary user). State transitions occur at the beginning of each slot with transition probabilities. Since the unavailability of a channel may also be caused by channel fading, the Markov chain model can also include fading statistics. If the primary traffic is modelled as a Markov chain, the secondary access opportunities can be estimated by stochastic learning techniques.

When the primary traffic is more dynamic and varying fast, like the cellular channel and the TV channel with the presence of wireless microphones, the Markov chain model may not be valid. And, when the cognitive networks

work in the unlicensed band, the traffic arrival from dissimilar networks will be more frequent and have less correlation. So, in this paper, we assume the arrival of the primary traffic to follow a Poisson process. But our solution can be easily adapted to the previous Markov chain model by computing the success probability P_{success} (defined in Section IV) by estimating the state of the Markov chain.

The maximum likelihood estimator for the Poisson arrival rate parameter λ_i is $\hat{\lambda}_i = 1/\bar{x}$, where $\bar{x} = \sum_{j=1}^n x_j$, $x = (x_1, \dots, x_n)$ are the n observations and n is the observation window size [18]. The arrival process can be nonstationary due to the complex arrival traffic, but we assume that within the GOP time duration, the arrival process follows a stationary Poisson process. During the operation, we can move the observation window to estimate the current λ .

B. Wireless Channel Error Rate Estimation

Different wireless channels may have different channel qualities in the sense of error probabilities. In this paper, we assume the selected subchannel has a packet loss probability π_i ($1 \leq i \leq S$). This π_i can be estimated either by pilot signals or by online stochastic learning as in [20].

The secondary users may not have the time, resources, or information for all the available channels for the PU traffic parameter and channel loss probability estimation. However, a distributive mechanism for these secondary users to exchange information will facilitate this estimation. Another method is an infrastructure-based secondary access, where there is a central station, and all the secondary devices report their observations to this station. Meanwhile, the station also broadcasts information about the channel availabilities and the estimated parameters to the secondary devices. Detailed protocols in these directions are beyond the scope of this paper, but we assume that the available channel set S_0 and parameters λ_i and π_i are known to the secondary devices.

IV. PROBLEM DESCRIPTION

The main problems addressed in this paper are as follows:

- determine the optimal number of subchannels S required to receive successfully a total N packets with high probability;
- determine the overhead (χ) such that $N = (1 + \chi)K$ for an SU link that maximizes the spectral efficiency of the distributed multimedia application with maximum tolerable delay D_{max} .

The GOP frame structure for our model is shown in Fig. 3. At the start of every GOP, the SU first performs sensing of the spectrum to find out the unused bands and then selects the required number of SCs from that pool to set up the secondary user link before starting the

transmission. Here T_{sensing} denotes the link setup time and D_{max} is the data transmission time.

Let P_{success} denote the probability that, for a secondary receiver, more than N packets are received successfully from S number of SCs. Then the spectral efficiency (η_{SUL}) for the SU link is given by

$$\eta_{\text{SUL}} = \frac{(1 - \epsilon)P_{\text{success}}K}{\text{SWT}_{\text{GOP}}} \quad (1)$$

where $T_{\text{GOP}} = T_{\text{sensing}} + D_{\text{max}}$.

Let the subchannel i have a loss probability π_i and PU arrival rate λ_i . Let each subchannel have the same channel capacity R_0 . Let the total number of packets to be transmitted per GOP from layer l be K^l and the total number of encoded packets needed for successful decoding of layer l be N^l . Then the total number of packets per GOP required for decoding is $N = \sum_{l=1}^L N^l$. We assume that packets from different layers are uniformly mixed in the same proportion as in the original source.

A. Subchannel Selection

Now suppose that the total number of available subchannels is S_0 . The SU needs to make a selection of $S \leq S_0$ SCs before starting our transmission. The optimal rate-allocation scheme as proposed in [10] states the following.

- As long as the channel with the highest quality can carry all the packets that are needed, all the packets are transmitted on that subchannel.
- The channel with the second highest quality is used only when the one with the highest quality has been exhausted.

In our scenario, there are two events that affect the quality of the SCs. A channel is considered good if PU arrives after the duration of one GOP and packets are not lost due to channel fading and noise. Since these two events are independent, we can multiply the probabilities of these two events and define a metric μ_i to measure the quality of the SCs as follows: $\mu_i = (1 - \pi_i)e^{-\lambda_i D_{\text{max}}}$. We use this metric to order the available SCs in the decreasing order of their quality so that if we require S number of SCs to establish the transmission link, then we just select the first S of the SCs from the pool of S_0 SCs. Since the required number of subchannels S depends on the required value of P_{success} , we first derive an analytical expression for P_{success} in terms of S .

B. An Analytical Expression for P_{success} : Analysis I

An analytical expression for P_{success} can be derived in the following manner.

Let the total number of packets needed to be received from all the layers and S SCs be N_0 . Let N_i

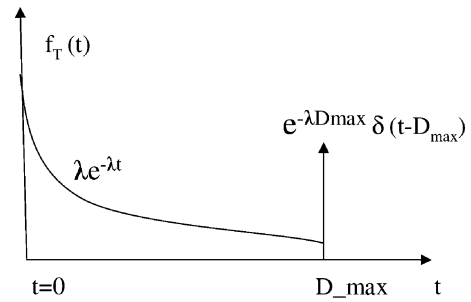


Fig. 8. Probability density function of T_i ($f_{T_i}(t)$).

be a random variable denoting the number of packets received on SC i . Then

$$P_{\text{success}} = P\left(\sum_{i=1}^S N_i \geq N_0\right) \quad (2)$$

where N_i is proportional to the available time on SC i denoted by a random variable T_i and is given by

$$N_i = \frac{(1 - \pi_i)RT_i}{D_{\text{max}}}, \quad i = 1, 2, \dots, S \quad (3)$$

and

$$T_i = \begin{cases} \tau_i, & \text{if } \tau_i \leq D_{\text{max}}, \\ D_{\text{max}}, & \text{if } \tau_i > D_{\text{max}} \end{cases} \quad (4)$$

where $\tau_i \sim \text{exp}(\lambda)$. Hence the probability density function (pdf) of T_i is given by

$$f_{T_i}(t) = \lambda_i e^{-\lambda_i t} [u(t) - u(t - D_{\text{max}})] + e^{-\lambda_i D_{\text{max}}} \delta(t - D_{\text{max}}) \quad (5)$$

where $u(n)$ is the unit step function and $\delta(t)$ is the Dirac delta function. Fig. 8 shows the pdf of T_i . After transforming T_i to N_i according to (3), the pdf of N_i is given by

$$f_{N_i}(n) = \frac{1}{A_i} \lambda_i e^{-\lambda_i n/A_i} [u(n) - u(n - A_i D_{\text{max}})] + e^{-\lambda_i D_{\text{max}}} \delta(n - A_i D_{\text{max}}) \quad (6)$$

where $A_i = (1 - \pi_i)R_0/D_{\text{max}}$.

Now, in order to compute P_{success} according to (2), we need to obtain the pdf of $\sum_{i=1}^S N_i$ by convolving the pdfs in (6) for $i = 1, 2, \dots, S$. Let the pdf of $\sum_{i=1}^S N_i$ be denoted by $f_N(n)$; then

$$f_N(n) = \bigotimes_{i=1}^S f_{N_i}(n) \quad (7)$$

where \otimes represents convolution. Now from (7) and (2), we can calculate the P_{success} as follows:

$$P_{\text{success}} = \int_{N_0}^{\infty} f_N(n). \quad (8)$$

C. An Analytical Expression for P_{success} : Analysis II

If we consider a more ideal case where all PU arrival rates λ_i are equal and the channel is free of error, then a closed-form solution for P_{success} can be derived in a manner similar to [12].

Here all SCs have the same channel capacity: R_0 packets per GOP and PU arrival rate λ . Then the total time (computed over all the SCs) needed to receive N_0 packets is $T_o = (N/R_0)T_{\text{GOP}}$. Let the i th PU arrive on SC i at τ_i ; then P_{success} is the probability that the total available time T computed over all the SCs before time D_{max} on each SC is greater than T_o .

For example, consider the case of three SCs as shown in Fig. 9. In Fig. 9(a), the total available time T , before time D_{max} on each SC, is $T = \tau_1 + D_{\text{max}} + \tau_3 = 5 + 10 + 8 = 23$, and in Fig. 9(b), it is $T = \tau_1 + \tau_2 + D_{\text{max}} = 6 + 2 + 10 = 18$. Now suppose the total time needed to receive N packets is $T_o = 20$; then N_0 packets are received successfully in Fig. 9(a) because $T > T_o$ while it results in a failure in Fig. 9(b) due to $T < T_o$.

Let C_r be a configuration as in Fig. 4, such that exactly r of the τ_i 's out of S are less than D_{max} and let T_r be a random

variable denoting the total available time (computed over all the SCs) in C_r . Then

$$P_{\text{success}} = \sum_{r=0}^S P(T_r > T_o | C_r) P(C_r) \quad (9)$$

and

$$P(C_r) = \binom{S}{r} (1-q)^r q^{S-r} \quad (10)$$

where $q = e^{-\lambda D_{\text{max}}}$ and

$$T_r = \begin{cases} (S-r)D_{\text{max}} + \sum_{i=1}^r \tau_i, & \text{if } r > 0 \\ SD_{\text{max}}, & \text{if } r = 0 \end{cases} \quad (11)$$

Let $(c-1)D_{\text{max}} < T_o \leq cD_{\text{max}}$ for some $c \in \{1, 2, \dots, S\}$; then

$$P(T_r \geq T_o | C_r) = \begin{cases} A_r, & \text{if } r > S - c \\ 1, & \text{if } r \leq S - c \end{cases} \quad (12)$$

where

$$A_r = P\left(\sum_{i=1}^r \tau_i \geq T_o - (S-r)D_{\text{max}} | C_r\right). \quad (13)$$

Since $\tau_i \sim \exp(\lambda)$ with pdf $p_{\tau_i}(t) = \lambda e^{-\lambda t} (t \geq 0)$, so the conditional pdf of τ_i given that $\tau_i \leq D_{\text{max}}$ is given by

$$p_{\tau_i}(t | \tau_i \leq D_{\text{max}}) = \frac{\lambda e^{-\lambda t}}{1-q}, \quad \text{where } (0 \leq t \leq D_{\text{max}}). \quad (14)$$

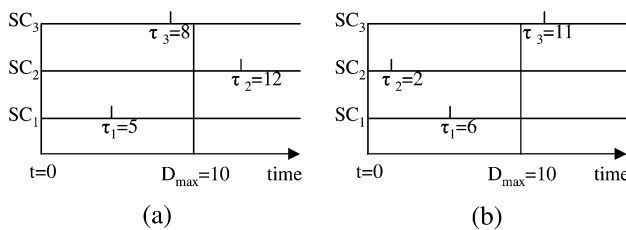


Fig. 9. Total available time T for two different configurations of τ_i 's.

Now since τ_i 's are identically distributed, the r -fold convolution of (14) gives the pdf of $\sum_{i=1}^r \tau_i$ (say, $p_r(t)$), given that $\tau_i \leq D_{\text{max}} \forall i$, which become r -times multiplication in the Laplace transform domain. Now taking the Laplace transform of (14), we get

$$\mathcal{L}[p_{\tau_i}(t | \tau_i \leq D_{\text{max}})] = \frac{\lambda}{1-q} \frac{1 - qe^{-sD_{\text{max}}}}{s + \lambda} \quad (15)$$

so

$$\mathcal{L}[p_r(t)] = \left[\frac{\lambda}{1-q} \frac{1 - qe^{-sD_{\max}}}{s + \lambda} \right]^r. \quad (16)$$

Now taking the inverse Laplace transform of (16), we get

$$p_r(t) = \alpha \sum_{i=0}^r \binom{r}{i} (-1)^i t^{*r-1} e^{-\lambda t} u(t^*) \quad (17)$$

where $\alpha = (1/(r-1)!)[\lambda/1-q]^r$, $t^* = t - iD_{\max}$, and $u(t)$ is a unit step function. Now from (13)

$$A_r = \int_{T_0 - (S-r)D_{\max}}^{\infty} p_r(t) dt \quad (18)$$

so (17) and (18) on simplification give

$$A_r = \frac{\sum_{i=0}^r \binom{r}{i} (-q)^i \Gamma(r, T^*)}{(r-1)!(1-q)^r} \quad (19)$$

where $\Gamma(r, t) = \int_t^{\infty} \tau^{r-1} e^{-\tau} d\tau$ is the complementary incomplete Gamma function and $T^* = \max[0, \lambda(T_0 - (S-r+i)D_{\max})]$. Now by combining (9), (10), (12), and (19), P_{success} can be computed.

Methods to compute LT decoding error probability (ϵ) have been proposed in [21] and [22], which we use in our simulations. We would like to optimize the spectral efficiency based on the following parameters:

- PU arrival rate (λ);
- Number of SCs available (S);
- Number of packets to be transmitted (K);
- Overhead required for LT decoding (χ).

Therefore, given λ and the delay constraint D_{\max} , we investigate the required number of SCs (S) and the overhead (χ) that will result in maximum spectral efficiency (η). Since computing a closed-form solution to this problem is combinatorially complex, we present some simulation results to illustrate the fundamental tradeoffs involved in this optimization problem.

V. SIMULATION RESULTS

For our simulation purposes, we make the following assumptions.

- Packets are lost only due to PU arrival, losses due to other channel conditions are not considered.

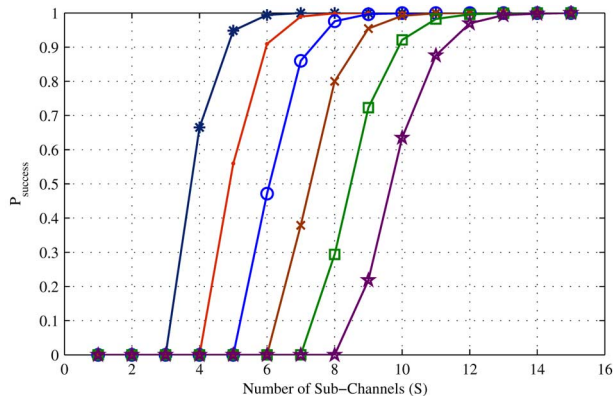


Fig. 10. Probability of successfully receiving more than N_0 packets (P_{success}) versus number of subchannels (S).

- There is no secondary user arrival.
- Once an SC is lost due to PU arrival, it is considered unusable during that GOP duration, i.e., even if the PU leaves the channel after some time, no further transmission is done until the next GOP.
- PU mean arrival time is comparable to the maximum tolerable delay (D_{\max}).

A. Parameterization

1) *Estimation of Number of Required Subchannels:* For the general case, where all SCs have different PU arrival rate and loss probability, Fig. 10 shows the dependence of P_{success} on the number of subchannels S for various values of N_0 with the following set of parameters: $R = 1000$ packets, $D_{\max} = 1$, $S_0 = 15$, and

$$\lambda = [0.3 \ 0.2 \ 0.1 \ 0.25 \ 0.36 \ 0.4 \ 0.6 \ 0.24 \ 0.32 \ 0.15 \\ 0.25 \ 0.36 \ 0.4 \ 0.6 \ 0.24]$$

$$\pi = [0.03 \ 0.04 \ 0.01 \ 0.02 \ 0.05 \ .025 \ 0.06 \ 0.01 \ 0.03 \\ 0.015 \ 0.04 \ 0.01 \ 0.02 \ 0.05 \ .025].$$

For example, if we need to receive $N_0 = 6500$ fountain coded packets at the receiver in order to recover an original $K = 6000$ packets with high probability of success, i.e., $P_{\text{success}} \simeq 1$, then at least $S = 10$ subchannels are needed, as shown in Fig. 10.

Simulations for the ideal case where all SCs have the same PU arrival rate with no channel loss is presented below.

2) *LT Codes:* For LT codes, the degree distribution $\Omega(k)$ that we use is the robust soliton distribution [15] and is

defined as follows. Let $R \equiv c \ln(K/\delta) \sqrt{K}$ for some suitable constants $c > 0$ and $0 < \delta \leq 1$. Define

$$\phi(k) = \begin{cases} (R/K)^{\frac{1}{k}} & \text{for } k = 1, 2, \dots, (K/R) - 1 \\ (R/K) \ln(\frac{R}{\delta}) & \text{for } k = K/R \\ 0 & \text{for } k > K/R \end{cases}$$

and $\beta = \sum_{k=1}^K [\phi(k) + \rho(k)]$, where $\rho(k)$ is the ideal soliton distribution given by

$$\rho(k) = \begin{cases} 1/K & \text{if } k = 1 \\ 1/k(k-1) & \text{for all } k = 2, 3, \dots, K' \end{cases}$$

Then $\Omega(k) = (1/\beta)[\phi(k) + \rho(k)]$.

In this paper, we take $c = 0.1$ and $\delta = 0.5$. The error probability ϵ , evaluated via simulation for various packet lengths K and overhead χ , is shown in Fig. 11. It is clear from Fig. 11 that for each value of K , ϵ becomes very small after certain overhead χ . It is also observed that as K increases, ϵ decreases for a fixed value of χ .

3) *Delay and Other Requirements*: The delay requirement for an MPEG-4 audio/video transmission is less than 150–400 ms [23]. In our simulation, we take $D_{\max} = 200$ ms. All SCs are assumed to have the same channel capacity $R_0 = 10$ Mbps with subchannel bandwidth $W = 100$ kHz. Packet size is $N_b = 1000$ bits per packet and T_{sensing} is assumed to be a constant (10 ms).

With the above parameters, the spectral efficiency η is evaluated for $K = 5000$ packets, various values of overhead χ , and the number of SCs (S). The results are plotted in Figs. 12–14 for different PU arrival rate λ .

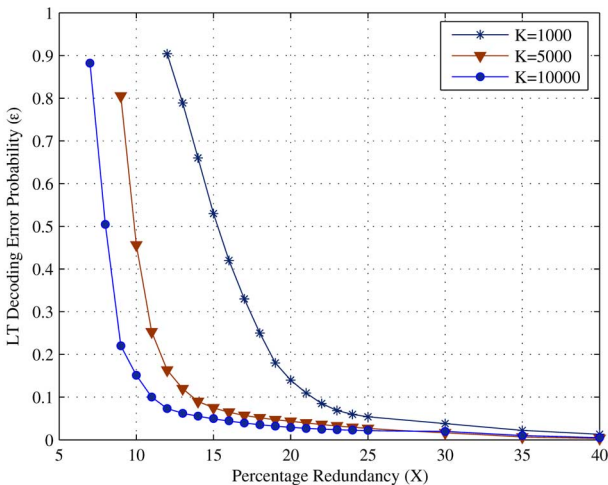


Fig. 11. LT decoding error probability.

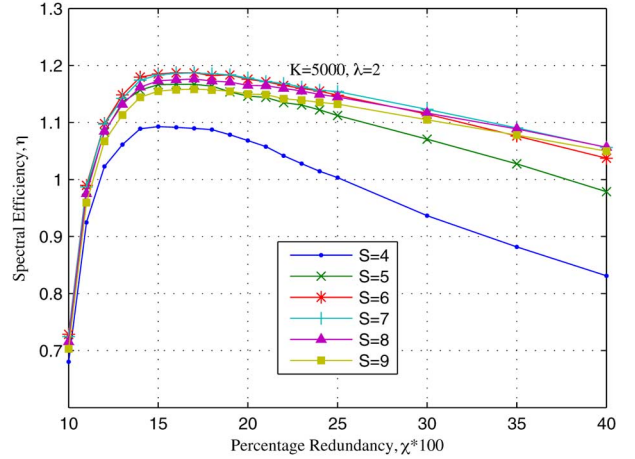


Fig. 12. Spectral efficiency for $K = 5000$ and $\lambda = 2$.

B. Performance Analysis

In Figs. 12–14, the spectral efficiency η , is plotted against the overhead χ , with number of subchannels S as a parameter, for $\lambda = 2, 5$, and 10 , respectively. From these figures, we make the following observations.

- For each value of S , η attains a maximum value at a specific value of χ .
- Moreover, η also attains another maximum at a specific value of S . For example, in Fig. 12, as S increases from four to nine, η initially increases and then decreases; it is maximum at $S = 6$. Similarly in Fig. 13, it is maximum at $S = 8$, and in Fig. 14 it is maximum at $S = 15$.
- By comparing the above three figures, we observe that η decreases as λ increases.

1) *Dependence on χ* : The spectral efficiency η initially increases with overhead χ . This is because a slight increase

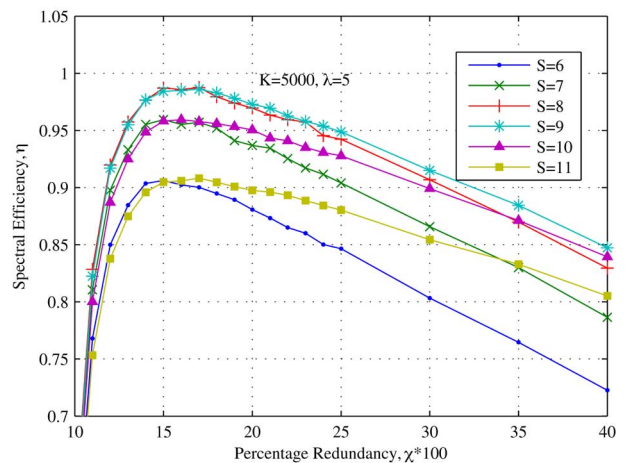


Fig. 13. Spectral efficiency for $K = 5000$ and $\lambda = 5$.

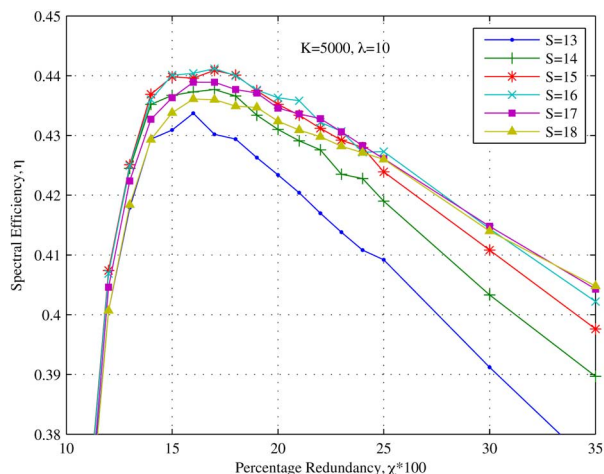


Fig. 14. Spectral efficiency for $K = 5000$ and $\lambda = 10$.

in χ causes a sharp decrease in LT decoding error probability ϵ (Fig. 11), resulting in an increase in η as seen from (1). But after a certain value of χ , ϵ becomes small and stable but an increase in χ increases N , the number of output packets to be received, which in turn increases T_{data} . This results in a decrease in η after a specific value of χ .

2) *Dependence on S*: Here, for a low value of S , the total time required per SC is large (i.e., T_{data} is large) and P_{success} is also low, both of which reduce η . But as S increases, P_{success} increases and becomes one after a certain value of S . Although T_{data} does decrease, causing a decrease in T_{frame} , this decrease is not fast enough compared to the increases in S due to a constant term T_{sensing} , so the increase in S dominates over the decrease in T_{frame} , causing η to decrease according to (1).

3) *Dependence on λ* : η monotonically decreases as λ increases because an increase in λ reduces the availability of the subchannel, thereby causing P_{success} to decrease and

T_{frame} to increase, both of which decrease the spectral efficiency according to (1).

By studying the various tradeoffs above, we see that for a given λ and number of original packets K , we can find out the value of the optimum number of SCs and the overhead that give maximum spectral efficiency.

VI. CONCLUSION

In this paper, we propose a scheme for the transmission of distributed multimedia applications over cognitive radio networks with the help of digital fountain codes. We model the primary user arrival as a Poisson process and discuss techniques to estimate the arrival rate. We propose a metric to measure the quality of the subchannels and then develop a scheme to select the required subchannels from the spectrum pool to establish the secondary user link. Then we investigate the problem of optimizing the spectral resources in the secondary usage scenario for multimedia applications with respect to the number of available subchannels and primary user occupancy of the subchannels. We also describe the use of the digital fountain codes to compensate for the loss incurred by the primary user interference and its effect on the spectral efficiency of the secondary user link.

We observe that there is an optimal number of subchannels that result in maximum secondary user spectral efficiency for same primary user traffic on all subchannels and for fixed parameters of the LT code. We also observe that there is an optimal LT code induced overhead that maximizes the secondary user spectral efficiency for a particular set of subchannels. And this efficiency monotonically decreases with the common primary user arrival rate for fixed LT code parameters and number of subchannels.

Future investigations in this area could include the multiple secondary user case and resulting interference issues. Other PU arrival models could be used to investigate the spectral efficiency. Additionally, other coding schemes can be used to investigate the link maintenance. ■

REFERENCES

- [1] Y. Xing, "Cognitive radio networks: Learning, games and optimization," Ph.D. dissertation, Dept. of Electrical and Computer Engineering, Stevens Inst. of Technology, Hoboken, NJ, 2006.
- [2] D. Cabric, S. M. Mishra, D. Willkomm, R. W. Broderon, and A. Wolisz, "A cognitive radio approach for usage of virtual unlicensed spectrum," in *Proc. 14th IST Mobile Wireless Commun. Summit 2005*, Dresden, Germany, Jun. 2005.
- [3] P. Kolodzy, "Spectrum policy task force: Findings and recommendations," in *Proc. Int. Symp. Adv. Radio Technol. (ISART)*, Mar. 2003.
- [4] M. McHenry, "Report on spectrum occupancy measurements," Shared Spectrum Company. [Online]. Available: http://www.sharedspectrum.com/?section=nsf_summary
- [5] Federal Communications Commission (FCC), Spectrum Policy Task Force, Nov. 15, 2002, ET Docket 02-135.
- [6] J. Mitola, "The software radio architecture," *IEEE Commun.*, vol. 33, no. 5, pp. 26–38, 1995.
- [7] SDR Forum, "Regulatory aspects of software defined radio," SDRF-00-R-0050-v0.0.
- [8] T. Weiss and F. Jondral, "Spectrum pooling: An innovative strategy for the enhancement of spectrum efficiency," *IEEE Commun. Mag.*, vol. 42, pp. S8–S14, Mar. 2004.
- [9] J. Apostolopoulos, T. Wong, W. Tan, and S. Wee, "On multiple description streaming with content delivery networks," in *Proc. IEEE Infocom 2002*.
- [10] J. Wagner, J. Chakareski, and P. Frossard, "Streaming of scalable video from multiple servers using rateless codes," in *Proc. IEEE Int. Conf. Multimedia Expo 2006*, Jul. 2006.
- [11] D. Willkomm, J. Gross, and A. Wolisz, "Reliable link maintenance in cognitive radio systems," in *Proc. IEEE Symp. New Frontiers Dyn. Spectrum Access Netw. (DySPAN 2005)*, Baltimore, MD, Nov. 2005.
- [12] H. Kushwaha and R. Chandramouli, "Secondary spectrum access with LT codes for delay-constrained applications," in *Proc. IEEE Consum. Commun. Network. Conf.*, Las Vegas, NV, Jan. 2007.
- [13] I. F. Akyildiz, W.-Y. Lee, M. C. Vuran, and S. Mohanty, "NeXt generation/dynamic spectrum access/cognitive radio wireless networks: A survey," *Comput. Netw.*, 2006.

- [14] J. Byers, M. Luby, M. Mitzenmacher, and A. Rege, "A digital fountain approach to reliable distribution of bulk data," in *Proc. ACM SIGCOMM 98*, Vancouver, BC, Canada, Jan. 1998, p. 5667.
- [15] M. Luby, "LT codes," in *Proc. 43rd Annu. IEEE Symp. Found. Comput. Sci. (FOCS)*, Vancouver, BC, Canada, Nov. 2002, pp. 271–280.
- [16] A. Shokrollahi, "Raptor codes," *IEEE Trans. Inf. Theory*, vol. 52, no. 6, pp. 2551–2567, Jun. 2006.
- [17] Q. Zhao, L. Tong, and A. Swami, "Decentralized cognitive MAC for dynamic spectrum access," in *Proc. IEEE DySPAN 2005*, Baltimore, MD, 2005.
- [18] S. M. Kay, *Statistical Signal Processing, Volume I: Estimation Theory*. Englewood Cliffs, NJ: Prentice-Hall, 1993.
- [19] C. Cordeiro, K. Challapali, D. Birru, and S. N. Sai, "IEEE 802.22: The first worldwide wireless standard based on cognitive radios," in *Proc. IEEE Conf. Dyn. Spectrum Access Netw. (DySPAN)*, 2005.
- [20] M. A. Haleem and R. Chandramouli, "Adaptive downlink scheduling and rate selection: A cross layer design," *IEEE J. Sel. Areas Commun. (Special Issue on Mobile Computing and Networking)*, Jun. 2005.
- [21] R. Karp, M. Luby, and A. Shokrollahi, "Finite length analysis of LT codes," in *Proc. ISIT 2004*, p. 37.
- [22] E. N. Maneva and A. Shokrollahi, *New model for rigorous analysis of LT codes*. [Online]. Available: <http://arxiv.org/abs/cs.IT/0512029>
- [23] 3GPP TSG-S4 Codec Working Group, "Error resilience in real-time packet multimedia payloads," 1999.
- [24] F. Campos, M. Karaliopoulos, M. Papadopoulou, and H. Shen, "Spatio-temporal modeling of traffic workload in a campus WLAN," in *Proc. 2nd Annu. Int. Wireless Internet Conf. (WICON06)*, Boston, MA, Aug. 2006.
- [25] S. Geirhofer, L. Tong, and B. M. Sadler, "A measurement-based model for dynamic spectrum access in WLAN channels," in *Proc. Military Communi. Conf. (MILCOM)*, Washington, DC, Oct. 2006.
- [26] N. S. Shankar, C. Cordeiro, and K. Challapali, "Spectrum agile radios: Utilization and sensing architectures," in *Proc. IEEE DySPAN*, 2005, pp. 160–169.

ABOUT THE AUTHORS

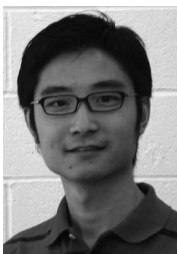
Harikeshwar Kushwaha (Student Member, IEEE) received the bachelor's degree from the Indian Institute of Technology, Kanpur, and the M.S. degree from the Electrical and Computer Engineering Department, Stevens Institute of Technology, Hoboken, NJ.

His research is in the area of cognitive radio networks.

Yiping Xing (Student Member, IEEE) received the B.S. degree from the University of Electronic Science and Technology of China, Chengdu, in 2001 and the M.E. degree from Stevens Institute of Technology, Hoboken, NJ, in 2004, both in electrical engineering. He received the Ph.D. degree from the Department of Electrical and Computer Engineering, Stevens Institute of Technology, in 2006.

His research interests include radio resource management for cellular and ad hoc networks, access control for cognitive radios, and game theory for wireless networks. He is currently with Bear Stearns.

Dr. Xing received the Outstanding Research Award in 2005 and the Graduate Fellowship Award in 2006 from Stevens Institute of Technology. He also received the IEEE CCNC 2006 Best Student Paper Award for his paper on dynamic spectrum access.



Rajarathnam Chandramouli (Senior Member, IEEE) is the Thomas E. Hattrick Chair Associate Professor of Information Systems in the Department of Electrical and Computer Engineering, Stevens Institute of Technology, Hoboken, NJ. His research in wireless networking and security, cognitive networks, steganography/ steganalysis, and applied probability is supported by the National Science Foundation, U.S. Air Force Research Laboratory, U.S. Army, Office of Naval Research, and other agencies.

Prof. Chandramouli is Founding Chair of the IEEE COMSOC Technical Subcommittee on Cognitive Networks and a Management Board Member of the IEEE SCC 41 standards committee.



Harry Heffes (Fellow, IEEE) received the B.E.E. degree from the City College of New York, New York, in 1962 and the M.E.E. and Ph.D. degrees in electrical engineering from New York University, Bronx, in 1964 and 1968, respectively.

He joined the Department of Electrical Engineering and Computer Science, Stevens Institute of Technology, Hoboken, NJ, in 1990. He became a Professor of electrical engineering and computer science after a 28-year career with AT&T Bell Laboratories (Bell Labs). In his early years with Bell Labs, he worked on the Apollo Lunar Landing Program, where he applied modern control and estimation theory to problems relating to guidance, navigation, tracking, and trajectory optimization. More recently, his primary concern has been with the modeling, analysis, and overload control of telecommunication systems and services. He is the author of papers in a broad range of areas, including voice and data communication networks, overload control for distributed switching systems, queuing and teletraffic theory and applications, and computer performance modeling and analysis. He was an Associate Editor of *NETWORKS: AN INTERNATIONAL JOURNAL*.

Dr. Heffes is a member of Eta Kappa Nu and Tau Beta Pi. He received the Bell Labs Distinguished Technical Staff Award in 1983 and, for his work on modeling packetized voice traffic, the IEEE Communication Society's S.O. Rice Prize in 1986. He was a U.S. Delegate to the International Teletraffic Congress. He has been listed in *American Men and Women of Science* and *Who's Who in America*.

